Phys. Status Solidi B **246**, No. 11–12, 2756–2759 (2009) / **DOI** 10.1002/pssb.200982284

physica status solidi b
www.pss-b.com
basic solid state physics

Investigation of the Aharonov–Bohm effect in a gated graphene ring

Magdalena Huefner*, Françoise Molitor, Arnhild Jacobsen, Alessandro Pioda, Christoph Stampfer, Klaus Ensslin, and Thomas Ihn

Solid State Physics Laboratory, ETH Zurich, Switzerland

Received 29 April 2009, accepted 25 June 2009
Published online 29 October 2009

PACS 73.20.−r, 73.22.−f, 73.23.−b, 73.61.Wp

* Corresponding author: e-mail huefner@phys.ethz.ch, Phone: ++41 44 63 33 767, Fax: ++41 44 63 31 146

We experimentally investigate the conductance of a single-layer graphene ring. The Aharonov–Bohm oscillation amplitude of the four-terminal resistance is very high with a visibility up to 10%. Additionally, we investigate the amplitude and the period of the Aharonov–Bohm effect over a magnetic field range of ±5 T. We find that, while the period remains constant, the amplitude rises by a factor of 2.

1 Introduction Since graphene has been isolated using mechanical cleavage for the first time [1, 2], rapid progress has been made concerning the fabrication of various nanostructures. Special interest has been put up to date on nanoribbons [3–5], constrictions [6–12], and quantum dots [13–15]. Despite the intensive research activities in the field of transport measurements through graphene nanostructures, graphene rings have received little experimental attention until now.

Nevertheless several inspiring theoretical papers addressing aspects closely related to the Aharonov–Bohm effect [16] in graphene systems have been published [17–20].

Recently the Aharonov–Bohm effect was investigated for the first time in a two-terminal ring-structure [21]. Here we present measurements with improved visibility of the Aharonov–Bohm oscillations and additional tunability of the ring structure smaller than that studied in Ref. [21]. The influence of in-plane gates on the AB-effect is studied in detail in Ref. [22].

2 Sample and characterization The substrate consists of a highly doped Si wafer topped with a 295 nm thick silicon oxide. Single layer graphene flakes were deposited by mechanical exfoliation employing the Scotch tape technique described in Ref. [1]. The flakes were located using optical microscope and potential candidates for single layer flakes were identified by the contrast of the image [2, 23]. To verify their single layer nature, we carried out Raman spectroscopy measurements [24, 25]. The flakes are subsequently patterned by two electron beam lithography (EBL) steps. In the first step the resist is patterned into the desired etch mask and the structure is transferred to the graphene by Ar/O_2 reactive ion etching, removing the unprotected graphene. A second EBL step is used to place the electrodes connecting source, drain, and the in-plane gates, which are fabricated by evaporating Cr/Au (2 nm/40 nm) [13, 14].

Figure 1a shows an atomic force micrograph of the sample on which the presented measurements were carried out. The area still covered with the single layer graphene sheet is seen in a lighter shade, whereas the area were the graphene has been removed by the etching process and the substrate can be seen appears almost black.

The graphene-ring has an inner radius of about 200 nm and an outer radius of about 350 nm. On both sides of the ring are two contacts, labeled C1 through C4 in Fig. 1a. This configuration allows to carry out four-terminal measurements. A back-gate (BG) can be used to tune the charge carrier density in the whole structure. The in-plane side-gate (SG) acts predominantly on one arm of the ring, inducing a controlled asymmetry in our system.

Figure 1b shows the four-terminal resistance of the sample at 500 mK and zero magnetic field over the BG voltage. After a bake out at 70 °C for several days the charge neutrality point is found at 15 V. We can see from this sweep that the potential landscape in this sample is different for electrons as for holes. We focus our measurements on the hole regime.

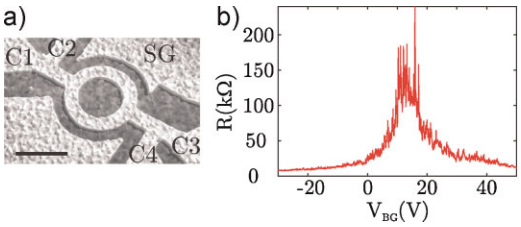

Figure 1 (online color at: www.pss-b.com) (a) Atomic force microscope image of the measured structure. The single layer graphene is seen in light gray, whereas the substrate is seen in a darker shade. The graphene ring has an inner diameter of 400 nm. The width of the arms is about 150 nm, thus avoiding the formation of undesired quantum dots in the arms. The four contacts of the ring are labeled C1 through C4. The side gate is marked with the letters SG and is located at a distance of 100 nm with respect to the sample. The scale bar has a length of 500 nm. (b) Back-gate sweep of the structure. The four-terminal resistance is recorded as a function of back-gate voltage V_{BG}. The measurement was carried out at a temperature of 500 mK at zero magnetic field. Zero volts were applied to the side-gate and a constant measurement current of 10 nA was used. The Dirac point is found at about 15 V.

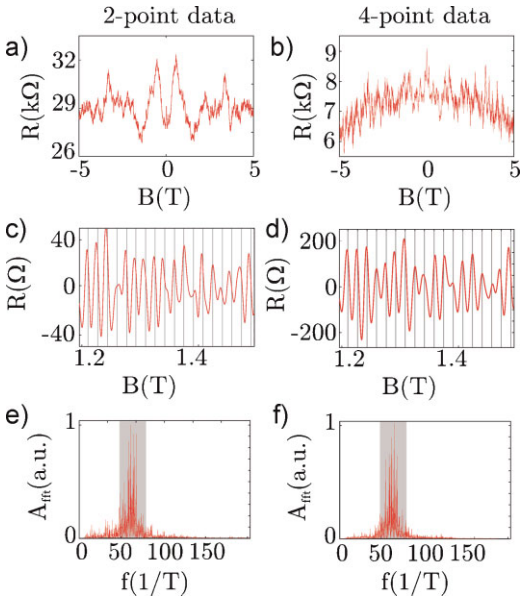

Figure 2 (online color at: www.pss-b.com) AB-oscillations measured over a large magnetic field range. The two-terminal case is shown in the left column, whereas the four-terminal data can be seen in the right column. (a) and (b) show the resistance traces as measured. Sub figures (c) and (d) show a zoom into the Aharonov–Bohm oscillations without the background resistance. It can be seen, that the oscillations are spaced with a period of 16 mT (indicated by the vertical gray lines). (e) and (f) show the fast Fourier transform of the traces shown in (a) and (b), respectively. A single peak at h/e can be observed. Since the $h/2e$ peak is missing, we estimate that the phase coherence length is smaller than twice the ring circumference. The gray underlined part represents the full width half maximum of the Fourier transform. Experimental settings: $V_{SG} = 0$ V and $V_{BG} = -30$ V, constant current = 5 nA.

When designing the ring we aimed to make the arms of the ring wide enough to avoid the localization of charge carriers observed in narrow graphene ribbons [6, 7]. However, thin arms are desirable to include as few radial modes as possible in transport. The width w of 150 nm is already small enough to lead to a relatively high resistance (200 kΩ) at the charge neutrality point [6]. The design was optimized in terms of the ratio r_0/w where r_0 is the average geometric radius, in order to separate the magnetic field scales of conductance fluctuations and the Aharonov–Bohm effect.

All measurements were carried out in a He^3 cryostat with a base temperature of about 500 mK. Standard low-frequency lock-in techniques were used to measure the resistance of the ring. All measurements shown here were recorded by applying a constant current. The magnetic field is applied out of plane. After stabilizing the sample at certain gate-voltage settings, it can be measured up to a couple of days without charge rearrangements.

3 Data analysis Figure 2a displays two-terminal resistance data as a function of magnetic field with $V_{SG} = 0$ V and $V_{BG} = -30$ V. The traces show Aharonov–Bohm oscillations with a period of about 16.5 mT, on top of a varying background resistance. The background can be seen to vary on a larger field scale than the Aharonov–Bohm oscillations.

In order to subtract the background the trace is transformed into Fourier space. The fast Fourier transform is multiplied with a filter function to distinguish the periodic Aharonov–Bohm oscillations from the background oscillations. The data is then transformed back into real space. This method is well established and described in more detail in Ref. [26].

Figure 2c shows a zoom into the periodic Aharonov–Bohm oscillations that are extracted from the raw data as described above.

4 Comparison of two-point and four-point measurements Figure 2 shows both the two-terminal measurement in sub figure (a) as well as the four-terminal measurement in (b). The overall resistance of the two-terminal measurement is about 20 kΩ higher than for the four-terminal measurement, consistent with the contact resistances.

Both traces show regularly spaced Aharonov–Bohm oscillations, which are displayed in 2c and d. The gray dashed lines have a spacing of 16.5 mT. This corresponds to a ring radius of 281 nm. This value is very close to the geometric average ring radius of 275 nm. The traces are symmetric with B in accordance with the Onsager theorem $R(B) = R(-B)$ valid for the two-terminal measurements [27–29]. The visibility is up to 10% for the four-terminal case and 3% in the two-terminal case.

The Fourier transforms are displayed in 2e and f. One single peak forms around 60 T^{-1} which corresponds to

17 mT. The width of the peak is $60 \pm 15\,\mathrm{T}^{-1}$. From the geometric dimensions of the ring, the Aharonov–Bohm period is expected to be 22 ± 11 mT which corresponds to $60 \pm 30\,\mathrm{T}^{-1}$. Therefore, the radius derived from the Aharonov–Bohm period lies well within the geometric dimensions of the structure. The position of the Fourier peak as well as the width are comparable for both the four-terminal and the two-terminal measurement.

The $h/2e$ peak in the Fourier spectrum which is expected around $120\,\mathrm{T}^{-1}$ is strongly suppressed. If we assume, that paths which are longer than the phase coherence length l_ϕ do not longer interfere, we estimate the phase coherence length to be below 2 μm.

5 Large magnetic field range Figure 3 shows the detailed analysis of the four-terminal data discussed in the section above in terms of the period ΔB and amplitude A of the Aharonov–Bohm oscillations.

The evaluation was carried out as follows. Starting from the Aharonov–Bohm oscillations without background, each extremal position was determined. The separation in magnetic field between two such resistance extrema was taken to be half the period ΔB of the Aharonov–Bohm oscillations. This period ΔB is plotted in Fig. 3a. We observe an average value of about 17 ± 6 mT (as indicated by the gray shaded area).

Subsequently the amplitude is derived by taking the absolute value of the difference in resistance of two adjacent extremal positions. The amplitude A versus magnetic field is plotted in Fig. 3b. Taking into account the Aharonov–Bohm oscillations of the complete magnetic field range of ±5 T, we see that the average oscillation amplitude rises with increasing magnetic field values by a factor of 3. Such an increase in A at high magnetic fields can also be seen in metallic rings. There it is usually attributed to scattering on magnetic impurities [30, 31].

We observe the same tendencies in the two-terminal data. This tendency is also observed by Russo et al. [21] for the two-terminal case.

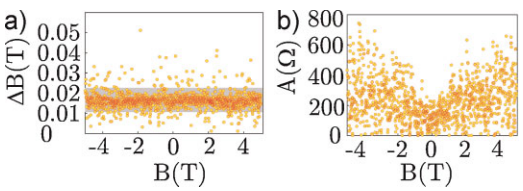

Figure 3 (online color at: www.pss-b.com) In this figure we show the analysis of the data shown in Fig. 2 in terms of frequency ΔB and amplitude A of the 4-point resistance data. Sub figure (a) shows the period of the Aharonov–Bohm oscillations. The gray shaded area corresponds to the marked area in the fourier spectrum seen in Fig. 2f. The period of the Aharonov–Bohm oscillations remains well within the range, that is, expected from the geometric dimensions of the ring. Furthermore, it remains constant over the complete investigated magnetic field range. The amplitude of the oscillation however, shown in (b) is seen to increase by about a factor of 3 over the investigated field range compared to 0 T.

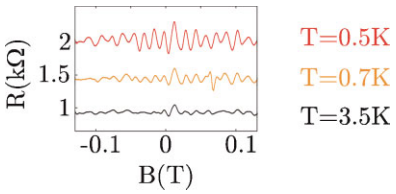

Figure 4 (online color at: www.pss-b.com) AB-oscillations with background subtracted for different temperatures. An offset is added to the data for clarity. The amplitude A decays with rising temperature.

6 Temperature dependence of the AB-oscillation amplitude Figure 4 shows the evolution of the Aharonov–Bohm oscillations with the background resistance subtracted for different temperatures. As the measurements were carried out in a He^3 system, only a limited temperature range down to 500 mK was accessible. We see that for this temperature regime the amplitude of the oscillations drops for rising temperature. This behavior is consistent with earlier findings [21] and can also be seen in metallic rings under certain conditions concerning the relative energy scales and the size of the phase coherence length [30].

We have shown above, that the amplitude of the Aharonov–Bohm oscillations rises at high magnetic fields. On the other hand it is known, that sweeping to high magnetic field can induce heating in the measurement system, which would in turn lead to a diminished oscillation amplitude. The rise in the amplitude of the Aharonov–Bohm oscillations seen at high magnetic fields (see Fig. 3) dominates over any such heating effects.

7 Conclusion We have investigated the Aharonov–Bohm effect in a side-gated single-layer graphene ring. We observe periodic Aharonov–Bohm oscillations with an amplitude up to 10% for the four-terminal measurement. The amplitude of the oscillations can be seen to rise at high magnetic fields, while the period remains constant. The radius derived from the ring oscillation period is in excellent agreement with the average geometric radius of the structure. The phase coherence length can be estimated from the suppression of the $h/2e$ period oscillations to be below 2 μm.

Acknowledgements We gratefully acknowledge support by the ETH FIRST lab and financial support from the Swiss Science Foundation (Schweizerischer Nationalfonds, NCCR Nanoscience).

References

[1] K. S. Novoselov, A. K. Geim, S. V. Morozov, D. Jiang, Y. Zhang, S. V. Dubonos, I. V. Grigorieva, and A. A. Firsov, Science **306**, 666 (2004).
[2] K. S. Novoselov, D. Jiang, F. Schedin, T. J. Booth, V. V. Khotkevich, S.V. Morozov, and A. K. Geim, Proc. Natl. Acad. Sci. USA **102**, 10451–10453 (2005).
[3] K. Wakabayashi, M. Fujita, H. Ajiki, and M. Sigrist, Phys. Rev. B **59**, 8271 (1999).

[4] K. Nakada, M. Fujita, G. Dresselhaus, and M. S. Dresselhaus, Phys. Rev. B **54**, 17954 (1996).
[5] V. Barone, O. Hod, and G. E. Scuseria, Nano Lett. **6**, 2748 (2006).
[6] F. Molitor, A. Jacobsen, C. Stampfer, J. Güttinger, T. Ihn, and K. Ensslin, Phys. Rev. B **79**, 075426 (2009).
[7] C. Stampfer, J. Güttinger, S. Hellmüller, F. Molitor, K. Ensslin, and T. Ihn, Phys. Rev. Lett. **102**, 056403 (2009).
[8] M. Y. Han, B. Ozyilmaz, Y. Zhang, and P. Kim, Phys. Rev. Lett. **98**, 206805 (2007).
[9] Z. Chen, Y.-M. Lin, M. J. Rooks, and P. Avouris, Physica E **40/2**, 228 (2007).
[10] K. Todd, H. Chou, S. Amasha, and D. Goldhaber-Gordon, Nano Lett. **9**, 1 (2009).
[11] X. Liu, J. B. Oostinga, A. F. Morpurgo, L. M. K. Vandersypen, ArXiv e-prints (arXivQ2:0812.4038), (2008).
[12] S. Schnez, F. Molitor, C. Stampfer, J. Güttinger, I. Shorubalko, T. Ihn, and K. Ensslin, Appl. Phys. Lett. **94**, 012107 (2009).
[13] C. Stampfer, J. Güttinger, F. Molitor, D. Graf, T. Ihn, and K. Ensslin, Appl. Phys. Lett. **92**, 012102 (2008).
[14] C. Stampfer, E. Schurtenberger, F. Molitor, J. Gűttinger, T. Ihn, and K. Ensslin, Nano Lett. **8**(8), 2378 (2008).
[15] L. A. Ponomarenko, F. Schedin, M. I. Katsnelson, R. Yang, E. H. Hill, K. S. Novoselov, and A. K. Geim, Science **320**, 356 (2008).
[16] Y. Aharonov and D. Bohm, Phys. Rev. **115**, 485 (1959).
[17] A. Rycerz, J. Tworzydlo, and C. W. J. Beenakker, Europhys. Lett. **79**, 57003 (2007).
[18] P. Recher, B. Trauzettel, A. Rycerz, Ya. M. Blanter, C. W. J. Beenakker, and A. F. Morpurgo, Phys. Rev. B **76**, 235404 (2007).
[19] A. Rycerz, Acta Phys. Pol. A **115**, 322 (2009).
[20] J. Wurm, M. Wimmer, H. U. Baranger, K. Richter, Semicond. Sci. Technol., Focus Issue on Graphene, in press, (arXiv:0904.3182), (2009).
[21] S. Russo, J. B. Oostinga, D. Wehenkel, H. B. Heersche, S. Shams Sobhani, L. M. K. Vandersypen, and A. F. Morpurgo, Phys. Rev. B **77**, 085413 (2008).
[22] F. Molitor, M. Huefner, A. Jacobsen, A. Pioda, C. Stampfer, K. Ensslin, T. Ihn, ArXiv e-prints (arXiv:0904.1364v1), (2009).
[23] P. Blake, E. W. Hill, A. H. Castro Neto, K. S. Novoselov, D. Jiang, R. Yang, T. J. Booth, and A. K. Geim, Appl. Phys. Lett. **91**, 063124 (2007).
[24] A. C. Ferrari, J. C. Meyer, V. Scardaci, C. Casiraghi, M. Lazzeri, F. Mauri, S. Piscanec, D. Jiang, K. S. Novoselov, S. Roth, and A. K. Geim, Phys. Rev. Lett. **97**, 187401 (2006).
[25] D. Graf, F. Molitor, K. Ensslin, C. Stampfer, A. Jungen, C. Hierold, and L. Wirtz, Nano Lett. **7**, 238 (2007).
[26] M. Sigrist, A. Fuhrer, T. Ihn, K. Ensslin, S. E. Ulloa, W. Wegscheider, and M. Bichler, Phys. Rev. Lett. **93**, 066802 (2004).
[27] L. Onsager, Phys. Rev. **37**, 405 (1931).
[28] L. Onsager, Phys. Rev. **38**, 2265 (1931).
[29] M. Büttiker, Phys. Rev. Lett. **57**, 1761 (1986).
[30] S. Washburn and R. A. Webb, Adv. Phys. **35**, 375 (1986).
[31] F. Pierre and N. O. Birge, Phys. Rev. Lett. **89**, 206804 (2002).